AD-A120 247 SOUTHERN METHODIST UNIV DALLAS TX DALLAS GEOPHYSICAL LAB F/G 8/11
PREDICTION AND ELIMINATION OF PRESSURE GENERATED GROUND NOISE O--ETC(U)
1977 E HERRIN, T GOFORTH F49620-76-C-0030
UNCLASSIFIED AFOSR-TR-82-0823 NL

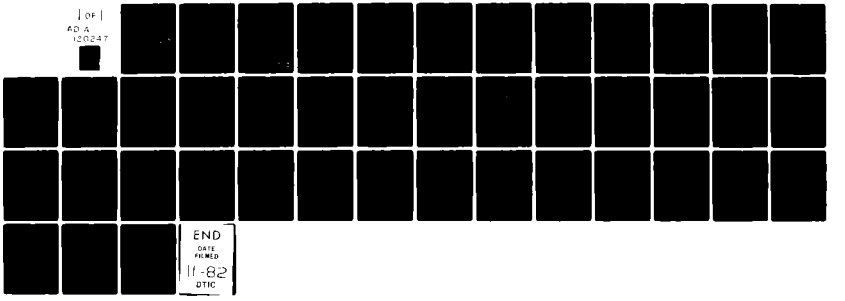

UNCLASSIFIED

SECURITY CLASSIFICATION OF THIS PAGE *(When Data Entered)*

(2)

REPORT DOCUMENTATION PAGE		READ INSTRUCTIONS BEFORE COMPLETING FORM
1. REPORT NUMBER **AFOSR-TR- 82-0823**	2. GOVT ACCESSION NO. AD-A120247	3. RECIPIENT'S CATALOG NUMBER
4. TITLE *(and Subtitle)* PREDICTION AND ELIMINATION OF PRESSURE GENERATED GROUND NOISE ON LONG PERIOD SEISMOGRAMS USING OPTIMUM FILTERS		5. TYPE OF REPORT & PERIOD COVERED INTERIM 6. PERFORMING ORG. REPORT NUMBER
7. AUTHOR(s) Eugene Herrin Tom Goforth		8. CONTRACT OR GRANT NUMBER(s) F49620-76-C-0030
9. PERFORMING ORGANIZATION NAME AND ADDRESS Dallas Geophysical Laboratory Southern Methodist University Dallas, Texas 75275		10. PROGRAM ELEMENT, PROJECT, TASK AREA & WORK UNIT NUMBERS 61102F 3291-40-30
11. CONTROLLING OFFICE NAME AND ADDRESS AFOSR/NP BOLLING AFB, DC 20332		12. REPORT DATE 1977 13. NUMBER OF PAGES 41
14. MONITORING AGENCY NAME & ADDRESS*(if different from Controlling Office)*		15. SECURITY CLASS. *(of this report)* UNCLASSIFIED 15a. DECLASSIFICATION/DOWNGRADING SCHEDULE

16. DISTRIBUTION STATEMENT *(of this Report)*

APPROVED FOR PUBLIC RELEASE; DISTRIBUTION UNLIMITED

DTIC ELECTE S OCT 14 1982 D B

17. DISTRIBUTION STATEMENT *(of the abstract entered in Block 20, if different from Report)*

18. SUPPLEMENTARY NOTES

19. KEY WORDS *(Continue on reverse side if necessary and identify by block number)*

20. ABSTRACT *(Continue on reverse side if necessary and identify by block number)*

Seismic noise generated by surface winds severely limits the usefulness of long-period seismograms. A linear dependence is observed between the recordings of a long-period seismograph and a co-located microbarograph in the period range 20 to 100 seconds. It is possible to design a filter, based on the least-mean-square method, such that the effects of the wind generated noise on the seismograph may be predicted from the atmospheric pressure changes recorded by microvarograph located at the same site. (over)

DD FORM 1 JAN 73 1473 EDITION OF 1 NOV 65 IS OBSOLETE

82 10 12 156

UNCLASSIFIED

SECURITY CLASSIFICATION OF THIS PAGE *(When Data Entered)*

20. (cont.)
The filter has been used to reduce the noise level for seismic data and hence increase the S/N ratio. However, only limited success has been achieved and the efficiency of the prediction tends to depend on the wind direction, wind speed and the variance of the wind speed. The turbulence cells associated with atmospheric pressure changes are believed to be broken down into smaller cells as the speed and variability of the wind increase. The increase of high frequency energy contributed by smaller cell disturbances also increases the nonlinear part of the transfer function and hence breaks down the prediction ability of the filter.

AFOSR-TR- 82-0823

(2)

SEMI-ANNUAL TECHNICAL REPORT

to the

AIR FORCE OFFICE OF SCIENTIFIC RESEARCH

from

Eugene Herrin

and

Tom Goforth

Dallas Geophysical Laboratory
Southern Methodist University
Dallas, Texas 75275

ARPA Order: 3291
Program Code: 7F10
Name of Contractor: Southern Methodist University
Effective Date of Contract: July 15, 1976
Contract Expiration Date: September 30, 1977
Total Amount of Contract Dollars: $194,755
Contract Number: F49620-76-C-0030
Principal Investigator and Phone Number: Eugene Herrin
AC 214 692-2760
Program Manager and Phone Number: Truman Cook, Director of
Research Administration
AC 214 692-2031
Title of Work: Propagation Path Effects for Rayleigh and
Love Waves
University Account Number: 80-88

Sponsored by
Advanced Research Projects Agency
ARPA Order No. 3291

PREDICTION AND ELIMINATION OF PRESSURE GENERATED GROUND NOISE ON LONG PERIOD SEISMOGRAMS USING OPTIMUM FILTERS

Jennifer Young, Eugene Herrin,
and Tom Goforth
Geophysical Laboratory
Southern Methodist University
March 1977

ABSTRACT

Seismic noise generated by surface winds severely limits the usefulness of long-period seismograms. A linear dependence is observed between the recordings of a long-period seismograph and a co-located microbarograph in the period range 20 to 100 seconds. It is possible to design a filter, based on the least-mean-square method, such that the effects of the wind generated noise on the seismograph may be predicted from the atmospheric pressure changes recorded by a microbarograph located at the same site. The filter has been used to reduce the noise level for seismic data and hence increase the S/N ratio. However, only limited success has been achieved and the efficiency of the prediction tends to depend on the wind direction, wind speed and the variance of the wind speed. The turbulent cells associated with atmospheric pressure changes are believed to be broken down into smaller cells as the speed and variability of the wind increase. The increase of high frequency energy contributed by smaller cell disturbances also increases the nonlinear part of the transfer function and hence breaks down the prediction ability of the filter.

TABLE OF CONTENTS

LIST OF TABLES

LIST OF ILLUSTRATIONS

INTRODUCTION

The background noise in the period range 20 to 100 seconds has always caused difficulties in the analysis of the surface wave data on long-period seismograms. A correlation has often been observed between changes in the magnitude of the long-period seismic noise and the atmospheric pressure fields. By studying the disturbances on the long-period vertical seismograph and the atmospheric pressure fluctuations on a nearby microbarograph, Crary and Ewing (1952) concluded that the correlation could be explained by atmospheric buoyancy effects on the seismometer. Great improvement in the performance of long-period vertical seismographs were obtained by elimination of buoyancy effects (Ewing & Press, 1953). Steps have been taken to avoid direct pressure effects, such as the seismometer being built in a tightly sealed, rigid steel case, which is then enclosed in a sealed steel vault. Still substantial correlation persists (Haubrich & Mackenzie 1965, Capon 1969) which is due to the elastic deformation of the ground caused by the atmospheric pressure changes.

Noise recorded by long-period seismometers consists of both propagating and non-propagating components (Ziolkowski,

1973). Rayleigh waves generated by sources such as the action of surf on the coast and from cultural activity are propagating noises. Approximately half the noise observed by long-period seismometers at LASA* (Capon, 1969) is non-propagating; that is, it is incoherent over distances of a few kilometers and is not of cultural or oceanic origin.

Previous studies have included mathematical models which describe the non-propagating component of the noise field. A plane pressure wave is assumed (Sorrells, 1971) to propagate at the mean wind speed over different models of layered half-spaces. These numerical studies indicate that pressure waves can contribute significantly to the output of the long-period vertical seismograph, and also create severe tilt noise on long-period horizontal seismographs. The pressure response of the earth tends to increase monotonically as the wavelength of the pressure oscillation increases. The seismic disturbances created by plane pressure waves decay rapidly with depth. Long-period seismographs have been situated both on the surface of the earth and in a mine at a depth of 183 meters at Grand Saline, Texas, by Sorrells et al (1971). The observations showed that during windy intervals, the local pressure change is strongly correlated with the

* Large Aperture Seismic Array (LASA), Billings, Montana

noise recorded on the surface and is incoherent with the noise recorded in the mine for the period range 20 to 100 seconds (Fig. 1). The ground noise on the long-period seismogram is thus of local origin, non-propagating and largely confined to the surface of the earth. Similar results have been obtained by Savino et al (1972) at a mine near Ogdensburg, New Jersey. The noise recorded in the mine remained a continuous low-level disturbance while the noise level on the surface varied by about 10 dB over a few days depending on the meteorological conditions. The wind generated noise attenuates rapidly with depth and can be virtually eliminated by installing the seismographs at a depth of several hundred meters (Sorrells 1971).

The coherence calculated from the recordings of a long-period seismograph and a nearby microbarograph indicates that there is a linearly dependent component between the two time series; therefore, it is possible to estimate the pressure generated earth noise by applying a linear transfer function to the microbarograph output. The transfer function, called a Wiener filter, is based on the least-mean-square method (Burg 1964). It has been applied to long-period seismic data by Ziolkowski (1973) and Douze et al (1975). Indiscriminant applications of the Wiener filter by these authors resulted in inconsistent results. In some cases, dramatic

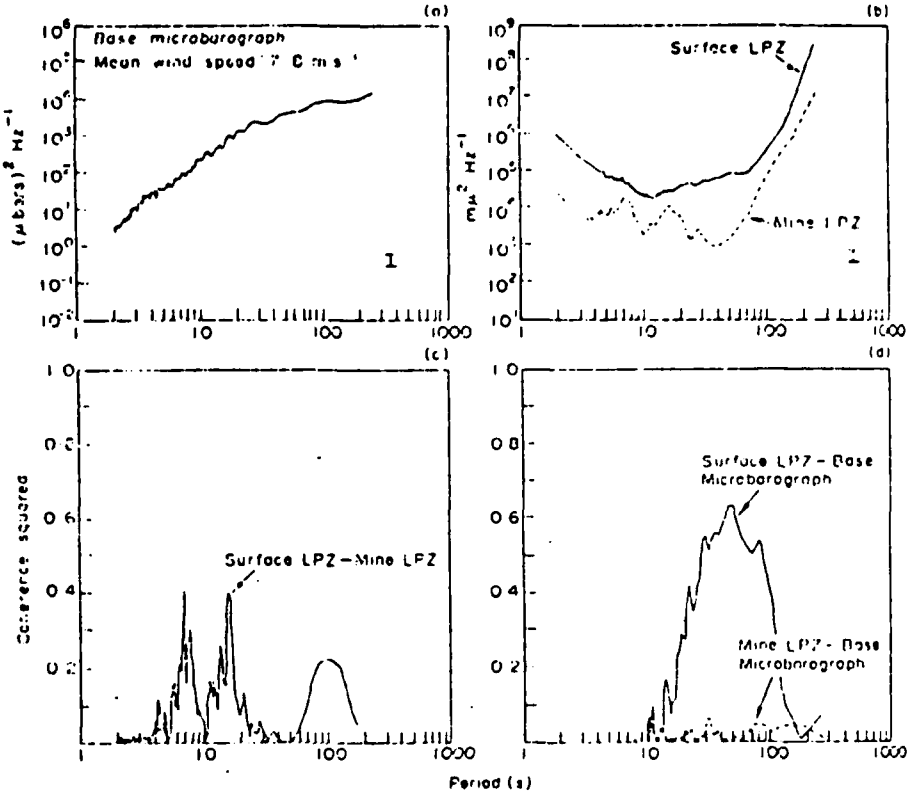

Fig. 1 Data recorded during a windy period with mean wind speed 7.8 m/s.

(a) Power spectrum of the noise recorded by base microbarograph.

(b) A comparison of the power spectral density estimates of the noise recorded by surface and mine vertical seismographs.

(c) Low coherence between surface and mine vertical seismographs.

(d) Base microbarograph is highly correlated to surface vertical seismograph and there is no coherence between base microbarograph and mine record. (from Sorrells et al 1971)

improvements in signal-to-noise ratio was achieved; in other cases, no improvements whatsoever resulted. It is the purpose of this study to identify the cause or causes of the inconsistent results, and to determine the optimum manner with which Wiener prediction filtering can be used with state-of-the-art long-period seismic recording.

NOISE PREDICTION TECHNIQUES

The noise caused by wind generated pressure changes recorded on long-period seismographs may be highly coherent with the microbarograph recordings at the same site when the wind blows strongly. The linear dependence between the outputs of the two instruments leads to the development of a filter which predicts the wind related noise in the seismic data. A Wiener filter, also known as an optimum shaping filter, is designed to produce a certain desired output from some input signal. In the case of this experiment, the noise data on the seismogram is the desired output for a shaping filter while the microbarograph data is the input signal. The filter is a linear system which best transfers the microbarograph signal to ground noise under the least mean square criterion. The mathematical operation is described in the following sections.

The output of the seismograph S(t) can be divided into two parts, N(t) and E(t). N(t) is the time series which is linearly related to the microbarograph output P(t), and is caused by local pressure fluctuations in the atmosphere. On the other hand E(t) is not linearly related to the pressure and contains noises generated from other sources and the

desired signals, thus

$$S(t) = N(t) + E(t) \qquad \text{(Eq. 1)}$$

Since N(t) is experimentally correlated with P(t), a Wiener filter F(t) can be determined by taking N(t) to be the desired output with input P(t); thus P(t) convolved with the filter yields $\hat{N}(t)$, an estimate of N(t).

$$P(t) * F(t) = \hat{N}(t) \qquad \text{(Eq. 2)}^{1}$$

To design the filter F(t), a time period should be chosen from intervals with high wind speed and no other obvious seismic signals so that most of the noise energy on the long-period seismogram is wind related; i.e. $E(t) \cong 0$. The seismic output S(t) in this time period is then approximately equal to wind noise N(t), the desired output for the shaping filter. Equations 1 and 2 can be written as

$$S(t) \cong N(t) \quad \text{and} \quad P(t) * F(t) = S(t)$$

Steps to generate the filter are described in detail by Kanasewich (1973) and Robinson (1967), and are summarized as follows.

Let microbarograph P(t) = input $\qquad t = 1,\ldots\ldots,T$

seismograph S(t) = desired output $\qquad t = 1,\ldots\ldots,T$

f(k) = unknown filter coefficients $\qquad k = 1,\ldots\ldots,K$

A(t) = output after filtering $\qquad t = 1,\ldots\ldots,T$

1. The symbol * indicates convolution.

The actual output A(t) is the convolution of microbarograph P(t) and the unknown filter f(k), that is

$$P(t) * f(t) = A(t)$$

$$A(t) = \sum_{k=1}^{K} f(k)\, P(t-k) \qquad t = 1,\ldots T+K-1$$

The error between A(t) and desired output S(t) is defined as

$$e(t) = A(t) - S(t)$$

$$e(t) = \left[\sum_{k=1}^{K} f(k)\, P(t-k)\right] - S(t) \qquad t=1,\ldots T+K-1$$

The errors are squared and summed for the time series as E.

$$e(t)^2 = \left\{\left[\sum_{k=1}^{K} f(k)\, P(t-k)\right] - S(t)\right\}^2$$

$$E = \sum_{t=1}^{T+K-1} e(t)^2$$

$$E = \sum_{t=1}^{T+K-1} \left\{\left[\sum_{k=1}^{K} f(k)\, P(t-k)\right] - S(t)\right\}^2$$

The filter is best fitted with minimum error if the partial derivatives of E with respect to each of the filter coefficients are equated to zero.

$$\frac{\partial E}{\partial f(j)} = 0 \qquad j = 1,\ldots\ldots,K$$

$$\frac{\partial E}{\partial f(j)} = 2 \sum_{t=1}^{T+K-1} \left\{ \left[\sum_{k=1}^{K} f(k)\, P(t-k) \right] - S(t) \right\} P(t-j) = 0$$

which gives $$\sum_{k=1}^{K} f(k) \left[\sum_{t=1}^{T+K-1} P(t-k)\, P(t-j) \right] = \sum_{t=1}^{T+K-1} S(t)\, P(t-j)$$

$$j = 1, \ldots, K \quad \text{(Eq. 3)}$$

where $\sum_{t=1}^{T+K-1} P(t-k)\, P(t-j) = \Phi_{j-k}$ is the autocorrelation of P(t) and

$\sum_{t=1}^{T+K-1} S(t)\, P(t-j) = C_{-j}$ is the crosscorrelation of S(t) & P(t).

By substituting Φ_{j-k} and C_{-j} into Eq. 3, we have

$$\sum_{k=1}^{K} f(k)\, \Phi(j-k) = C(-j) \qquad j=1,\ldots,K \quad \text{(Eq. 4)}.$$

Hence the desired filter coefficients are calculated by using the autocorrelation of microbarograph and the cross-correlation of microbarograph and seismic noise data. Eq. 4 represents a set of K simultaneous equations and can be written out in the matrix form,

$$\begin{bmatrix} \phi(0) & \phi(1) & \ldots & \phi(k-1) \\ \phi(1) & \phi(0) & \ldots & \\ & & & \\ \phi(k-1) & \ldots & & \phi(0) \end{bmatrix} \begin{bmatrix} f_1 \\ f_2 \\ \\ f_k \end{bmatrix} = \begin{bmatrix} C_1 \\ C_2 \\ \\ C_k \end{bmatrix}$$

The K filter coefficients are unknown and can be calculated by inverting the KxK matrix, but the computation work is great for a large number of filter coefficients. The problem is simplified by using the recursive method first introduced by Levinson (1947), in which one solves the equations in a step-wise manner. We start by computing a one-point filter, and then the steps for filters with 2, 3, ..., K points are calculated successively. The machine time required to solve the simultaneous equations for a filter with K coefficients is proportional to K^2 using the recursive method, as compared to K^3 using the conventional method. The computer storage space is also condensed by using this recursive method.

An infinitely long filter is required to produce exactly a desired output and it follows that E decreases as filter length increases. The error of the filter is computed at each filter length during the iteration, and usually the error will decrease rapidly and then level off. The least number of filter points required for minimum error can be determined by experiment.

The Wiener filter is then applied to a time period of interest which is within two or three hours of the time period from which the filter was obtained. The wind-related noise N(t) can be estimated by convolving the microbarograph output with the filter to obtain $\hat{N}(t)$. Subtracting $\hat{N}(t)$ from the

seismic data S(t) yields an improvement in signal-to-noise ratio, providing that the linearly dependent portion of the noise field is significant.

EXPERIMENTS AND RESULTS

The site of the experiments was McKinney, Texas, about 30 miles north of Dallas. At McKinney, seismic and meteorological data were recorded continuously on thirty-two channels of digital, magnetic tape. Channels containing data from the long-period vertical, long-period E-W, long-period N-S seismographs; and the microbarograph and wind speed and wind direction indicators were used in this experiment. The wind speed in the McKinney area during the year 1974 was generally low. Prolonged periods of wind speeds in excess of 5 meters/second (about 11 miles/hr) were rare.

Most of the earthquakes recorded at McKinney with magnitudes (m_b) greater than 4.5 show good Rayleigh wave dispersion patterns on the long-period vertical component (Fig. 2), but well dispersed Love waves are much more difficult to observe. Surface horizontal seismographs are much more susceptible to wind-generated noise than are vertical instruments and as a result generally exhibit a much higher noise level. The flat dispersion curve within the pass band of the instrument for oceanic Love waves results in a poorly dispersed wave which does not contrast greatly with the noise. Nevertheless, several examples were obtained.

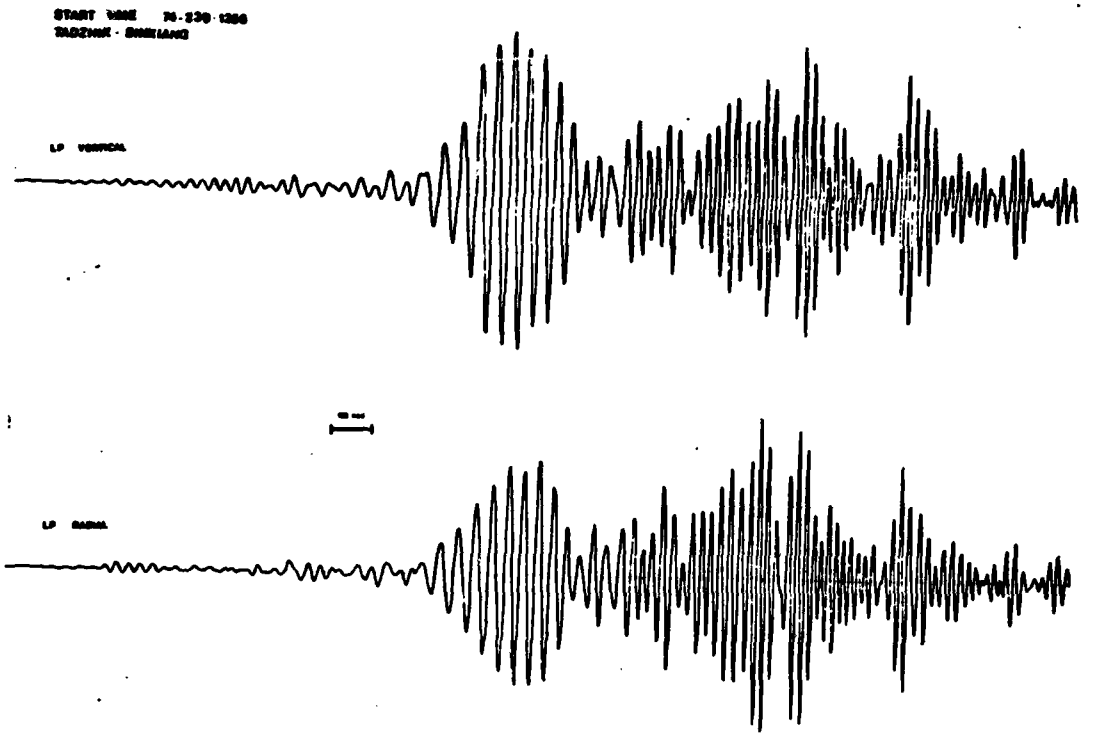

Fig. 2. Example of Rayleigh wave dispersion on vertical and radial directions for earthquake at TADZHIK-SINKIANG, N39.7, E73.8; m_b = 5.8, Depth = 33 km, Distance = 106°, Azimuth = 7.7°.

As noted previously, the noise related to the atmospheric effects is dominated by quasi-static deformations in response to wind generated pressure changes during windy intervals with moderately high wind speed (>4 m/s) (Douze et al, 1975). The wind moving over the surface also causes tilts on the horizontal components which depend on the wind direction.

The Preliminary Determination of Epicenters (PDE) of the USGS and the meteorological data for McKinney during the year 1974 were reviewed. Seventeen earthquakes were selected which were recorded during different conditions of wind speed and variability. Suitable filters were designed and applied to each event. The details of the filter design and the data processing is described in Fig. 3. The magnitudes (m_b) of the events selected ranged between 5.0 and 6.0. A period of noise data within three hours before or after the signal with similar wind conditions was selected for filter design. PDE sheets were checked to assure that no small events were included in the noise sample. The 3-component data were rotated for each event so that the horizontal seismographs were effectively oriented along directions radial and transverse to the travel path. Both earthquake and noise data were rotated and a Wiener filter was designed for each channel using the microbarograph data as an input. The output of the filter design program shows the error of the prediction. An

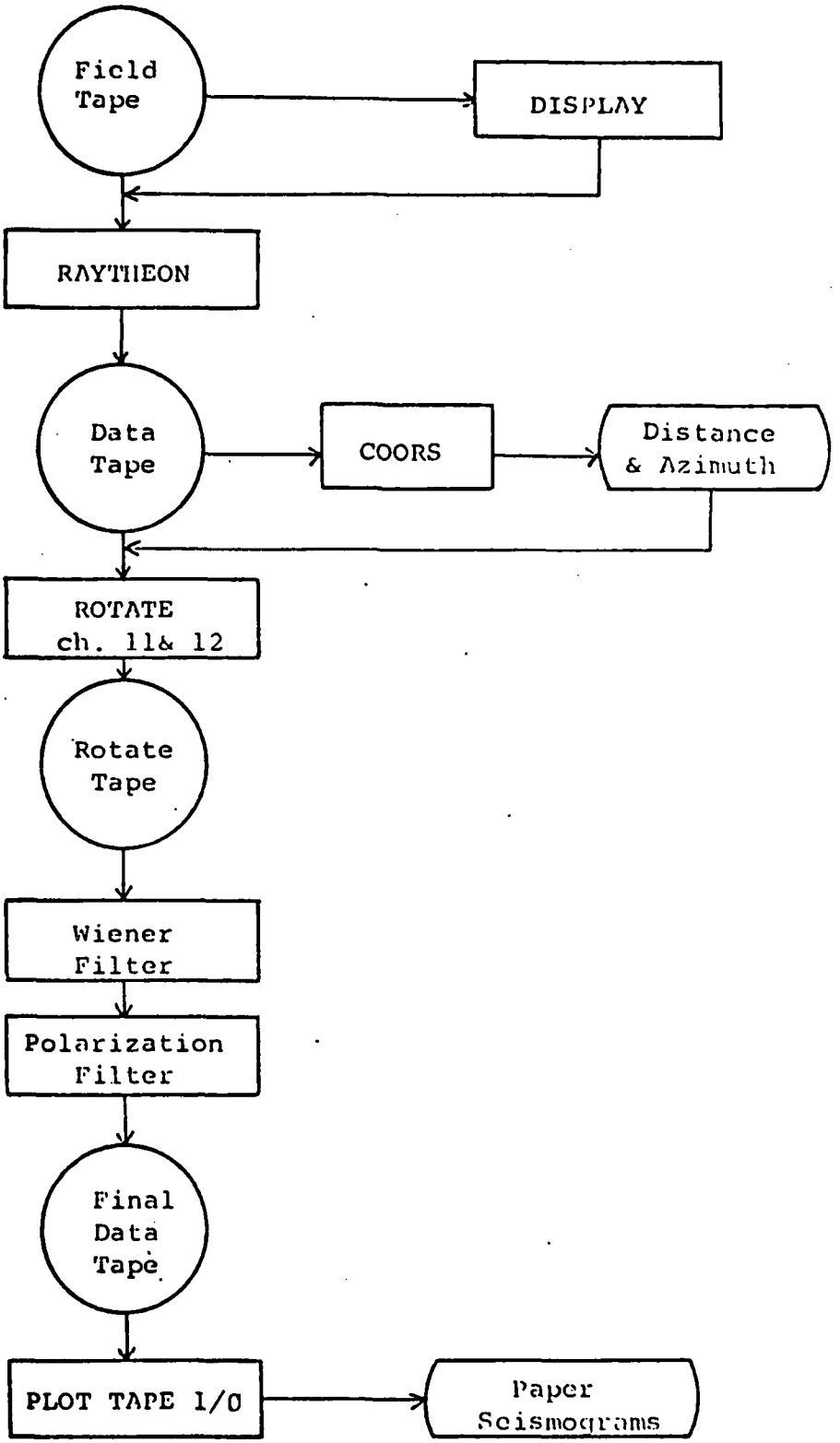

Fig. 3. Diagram showing the procedure for improvements of S/N ratio of surface waves. See Appendix for the program names.

error less than 0.50, which means more than 50% of the noise energy is predicted, is considered to be acceptable. Table 1 shows some of the results for earthquakes using Wiener filtering. The errors for all three rotated components are included. Event 0061 which is an earthquake in the Solomon Islands with magnitude 5.2 has an acceptably low prediction error, 0.178 on the transverse direction. Fig. 4 shows the seismograms before and after Wiener filtering. There is a large reduction in the noise level, and the presence of a Love wave signal can be recognized on the filtered transverse record.

All the other examples show poorer prediction of the noise energy on one or more channels. Several reasons for the failure of this approach are suggested.

1. Douze and Sorrells (1975) found that the prediction capability increased with the mean wind speed and the Wiener filter was most effective when the wind speed was greater than 5 m/s.

2. When high wind velocity prevails, the variability of the wind speed and direction may reduce filter effectiveness.

An effort was made to determine if the above suggestions were valid, and if so, to determine the conditions of wind speed and variability where Weiner filtering can be expected

Table 1. Prediction errors on three rotated channels for earthquake data

Event	Day-time	Angle (Deg) rotated	Wind dir.	Wind speed (M/S)	Prediction error V	Prediction error T	Prediction error R
0008	118-1930	275	S	6.5	.754	.740	.898
0015	116-2250	11.3	S	5.8	.739	.789	.649
0019	119-1417	301	S	6.9	.523	.615	.691
0050	131-1653	302	NE	4.2	.767	.648	.858
0061	136-0630	268	S	6.2	.352	.178	.487
0068	255-1100	155	S	4.5	.678	.325	.228
0069	264-0900	277	NE	4.5	.413	.251	.314
0070	264-2200	150	NE	4.5	.336	.465	.582
0071	265-1500	304	E	4.5	.337	.831	.809
0072	151-0300	2.9	S	5.6	.341	.487	.241
0073	118-1240	21.4	S	6.0	.552	.763	.626
0074	118-1640	251	S	5.6	.848	.892	.941
0075	118-2300	305	S	6.8	.682	.870	.856
0076	151-0210	314	S	5.6	.429	.389	.318

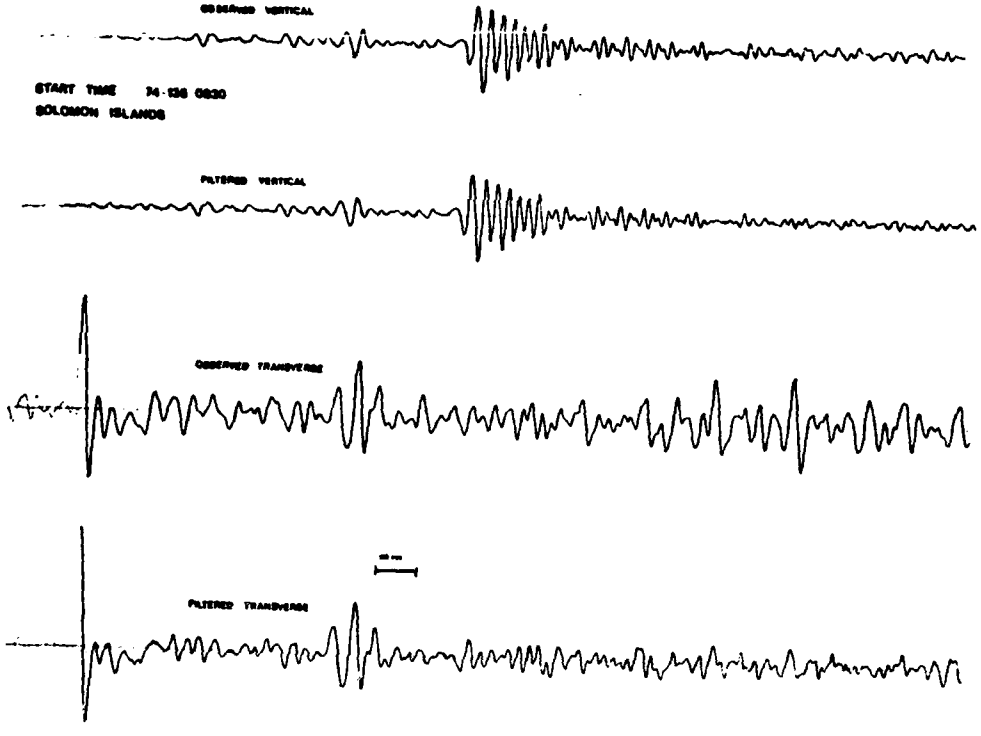

Fig. 4. The improvement of S/N ratio on transverse component for earthquake at Solomon Islands, S10.4, E161.1; Start time: 74-136-0756, m_b = 5.2, Depth = 77 km, Distance = 105.8°, Azimuth = 267.8°.

to be effective. Additional noise data were collected and the filter along with the prediction error for each channel was generated. Again, each noise sample was carefully chosen to exclude any identifiable small signals, propagating noise, or instrumental malfunction. Table 2 shows the result of the experiment, including the wind speed and its standard deviation. All the noise data used for prediction are 1024 seconds long, and the length of the filter is 232 points. Among most of the examples, the prediction on the horizontal components is better than that of the vertical component. This was not unexpected because horizontal seismographs are more susceptible to wind related earth tilts (Sorrells, 1971; Sorrells and Goforth, 1973) which cause larger apparent displacements at periods greater than 20 seconds than are seen on the vertical component. The tilting effects caused by the pressure changes also depend on the wind direction (Sorrells and Goforth, 1973). It can be seen from Table 2 that lower prediction errors for the horizontal channels always occur with the instruments aligned more nearly in the direction of the wind. An example of noise reduction is shown in Fig. 5.

Fig. 6 shows the plot of the percentage of total energy of the noise that can be predicted on the horizontal channels versus the average wind velocity. The percentage of noise prediction is calculated by one minus the average prediction

Table 2. Wind speeds, wind speed deviations and prediction errors for noise data

Event No.	Start Day-time	Angle (Deg) Rotated	Wind Speed (M/S) Dir.	Ave.	Dev.	Prediction Errors Ch.9 Z	Ch11 H	Ch12 H
01	121-0900	148	S	0.47	0.35	.875	ND	.875
02	125-0417	258	NE	3.25	0.57	.701	.438	.489
03	126-0738	250	N	1.00	0.22	.825	.760	.779
04	127-0954	149	N	0.41	0.50	.794	.692	.559
05	131-1653	302	NE	2.92	0.71	.767	.648	.858
06	136-0630	268	S	6.94	1.20	.352	.178	.487
07	140-2233	310	S	5.46	0.94	.558	.566	.396
08	151-0210	314	S	5.88	0.83	.429	.389	.318
90	151-0300	2.9	S	5.97	0.74	.341	.487	.241
10	255-1100	155	S	3.27	0.37	.678	.325	.228
11	264-0900	277	NE	3.78	0.68	.413	.251	.314
12	264-2200	150	NE	3.68	0.98	.336	.465	.582
13	51-0700		S	6.82	0.99	.286	.221	.166
14	51-1300		S	6.58	0.99	.457	.279	.148
15	77-0500		S	5.77	0.60	.280	.251	.178
16	77-0600		S	5.76	0.57	.323	.241	.293
17	136-0425		S	7.03	0.84	.573	.608?	.175

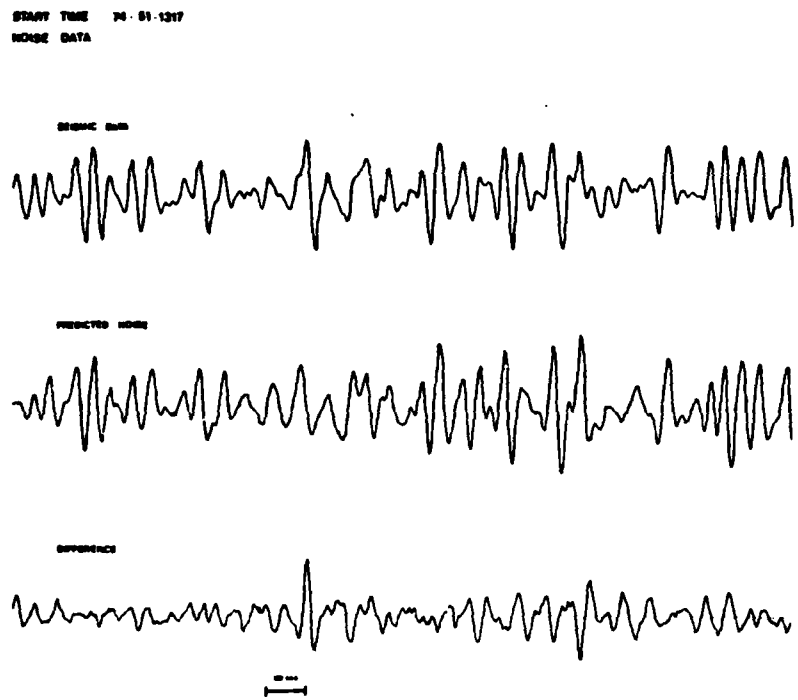

Fig. 5. Example of noise energy predicted from micro-barograph and noise data. The Wiener filter is used to estimate the noises on the noise data which generate the filter. The maximum amplitudes of all three figures are in the same scale. The wind was 6.58 m/s from the south. The prediction error on N-S direction is 0.148.

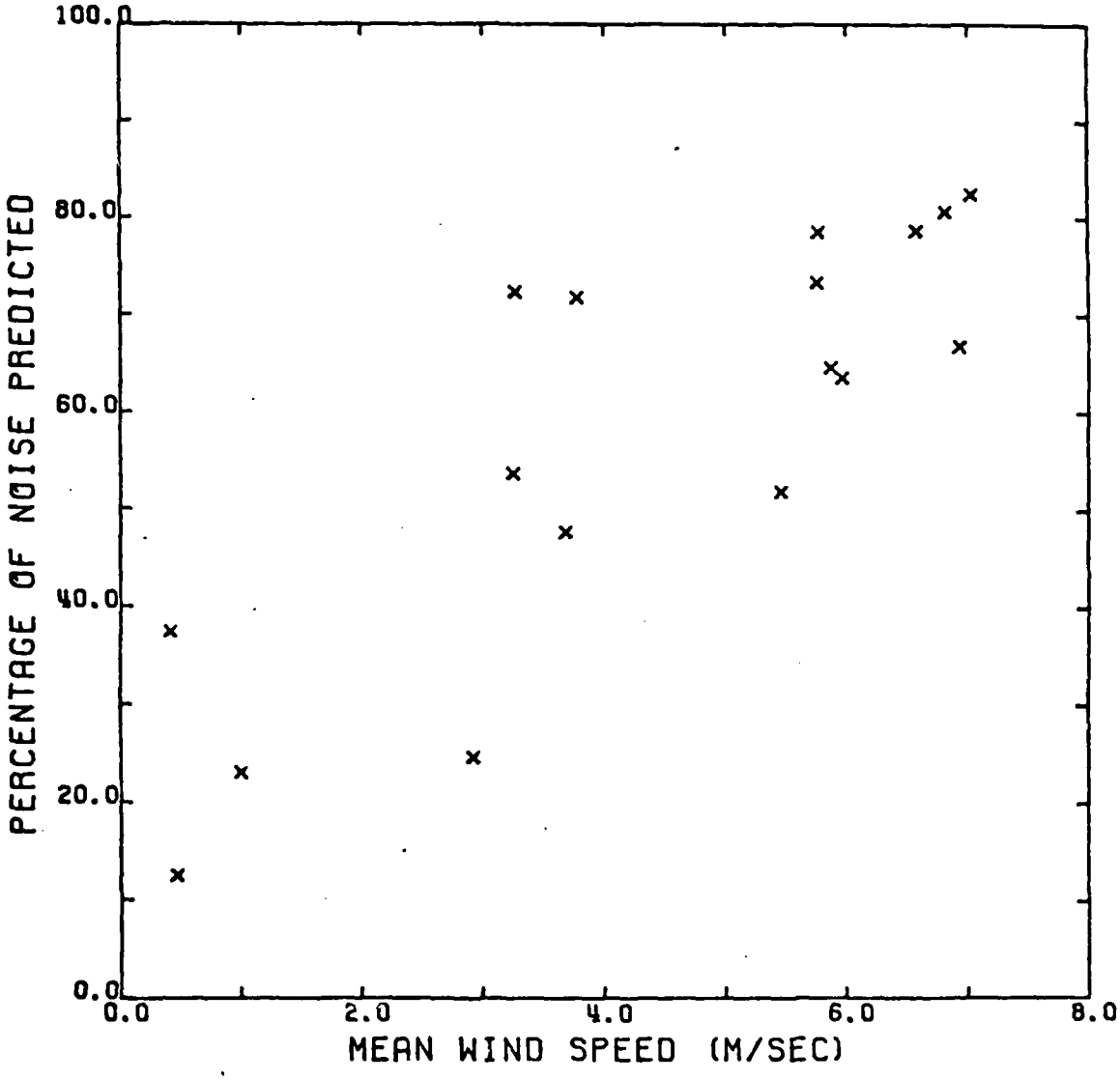

Fig. 6. The percentage of noise energy predicted on horizontal components versus the mean wind speed.

error for the two horizontal instruments. The predictions are scattered and the scatter increases with increasing wind speed. The scattering effect is shown to be caused by the variability of the wind speed about the mean in Fig. 7. Fig. 7 is a plot of the percentage of prediction versus the standard deviation of mean wind velocity. The numbers represent the mean wind speed for each event. The dashed lines are connected for points with wind speed of 3-4 m/s, 5-6 m/s, and 6-7 m/s respectively. It seems that the wind noise prediction from Wiener filtering is not only a function of the mean wind speed, but also a function of the deviation about the mean of the wind speed. The prediction error is small for each velocity category for a low variance of velocity but the error increases rapidly with increasing deviation in velocity. The higher the wind speed, the larger the deviation of wind speed permissable for successful Wiener filtering.

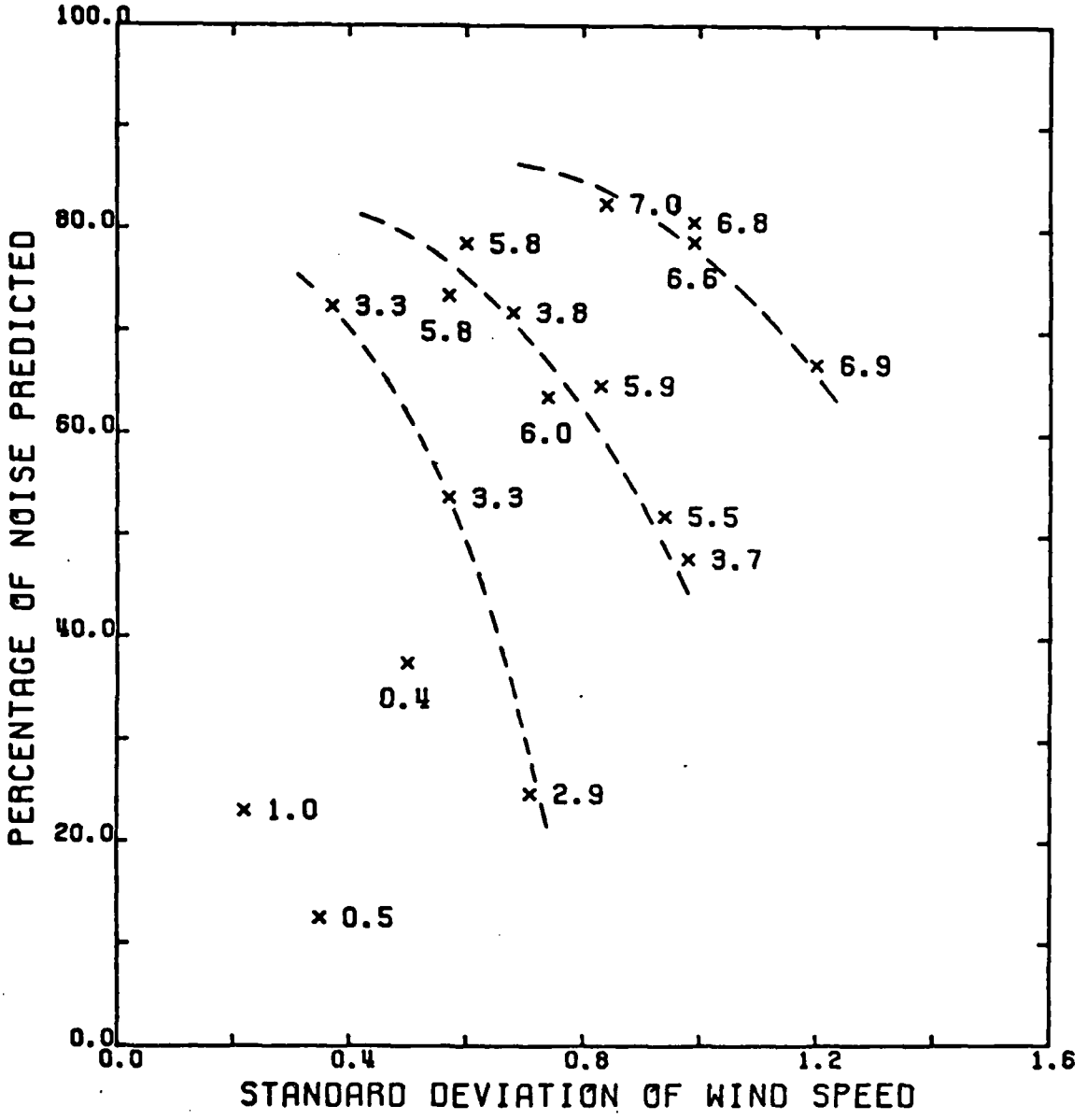

Fig. 7. The percentage of noise energy predicted on horizontal components versus the standard deviation of mean wind speed. The numbers in the figure show the mean wind velocity in meters/second for each event. Dash lines are connected by points of velocity 3-4m/s, 5-6 m/s, and 6-7 m/s respectively.

DISCUSSION

From the experimental data of J. McDonald and E. Herrin (1975), it is shown that there is a relationship between the measured wind speed and the associated micropressure level (Fig. 8). The pressure energy increases as the wind speed increases, and the resulting non-propagation contribution to the long-period seismic noise field constitutes a greater percentage of the total noise field. Thus, in general, the harder the wind blows, the more effective Weiner filtering will be.

The wind, which is the motion of the air in the boundary layer of the earth caused by the atmospheric pressure changes, is turbulent and consists of turbulent cells of all dimensions (J.A. McDonald et al, 1971). The bigger cells cause seismic background noise in the longer period range, while the smaller cells cause noise in the shorter period range. The turbulence has a wide range of subsidiary motions with different scale lengths and the energy is continuously passing from the larger to the smaller scale lengths. A large scale motion in the atmosphere is unstable and breaks down to motions of smaller scale length; that is, to smaller eddies.

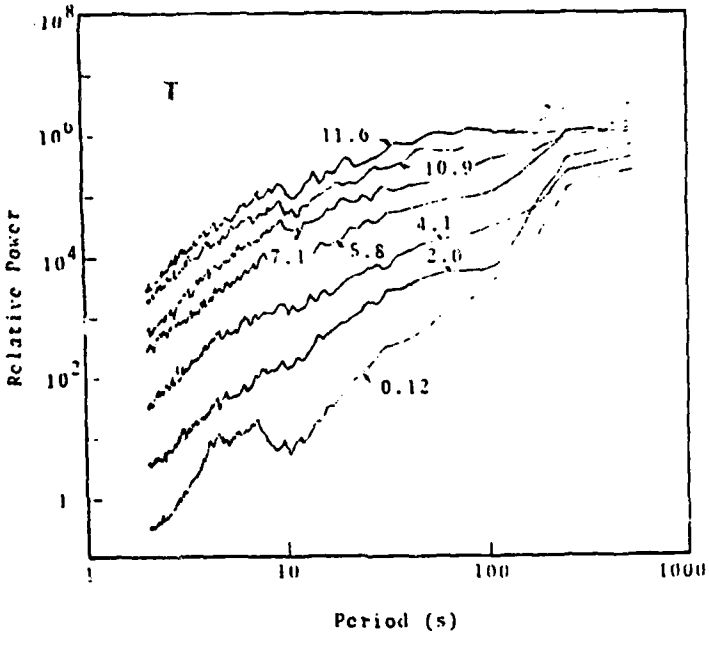

Fig. 8. The relative change in micropressure power estimates for different wind speed. The numbers indicate the average wind speed (m/s) during each data sample. (from McDonald et al 1975)

In Fig. 9, the power spectra of micropressures recorded during different wind conditions have been plotted. The wind speeds are approximately 5.7 m/s for figure (a) and 6.5 m/s for figure (b). In both plots, the high frequency component of the energy is most affected by a high variance of wind speed, B and D. The increase of high frequency energy reduces the fraction of the energy in the pressure field which is linearly related to the seismic noise. The high frequency disturbances associated with the small scale motions in the atmosphere thus interfere with the prediction of ground noise.

The linear coherence of the energies of two time series indicates that part of one time series is linearly dependent on the other time series while the whole process relating them might be a non-linear one (Ziolkowski, 1973). In other words, the linear component of one time series can be transformed from the other with a linear time-domain filter. The design of the Wiener filter is based on the linear dependence between the ground noise and microbarograph output in the period range 20 to 100 seconds. In a situation with variable wind, the high frequency energy will dominate the total energy spectrum of the microbarograph (Fig. 9). The increase of high frequency energy, which is also the incoherent part of the transform process, degrades the linear relation between the two time series, and hence causes increasing prediction error with

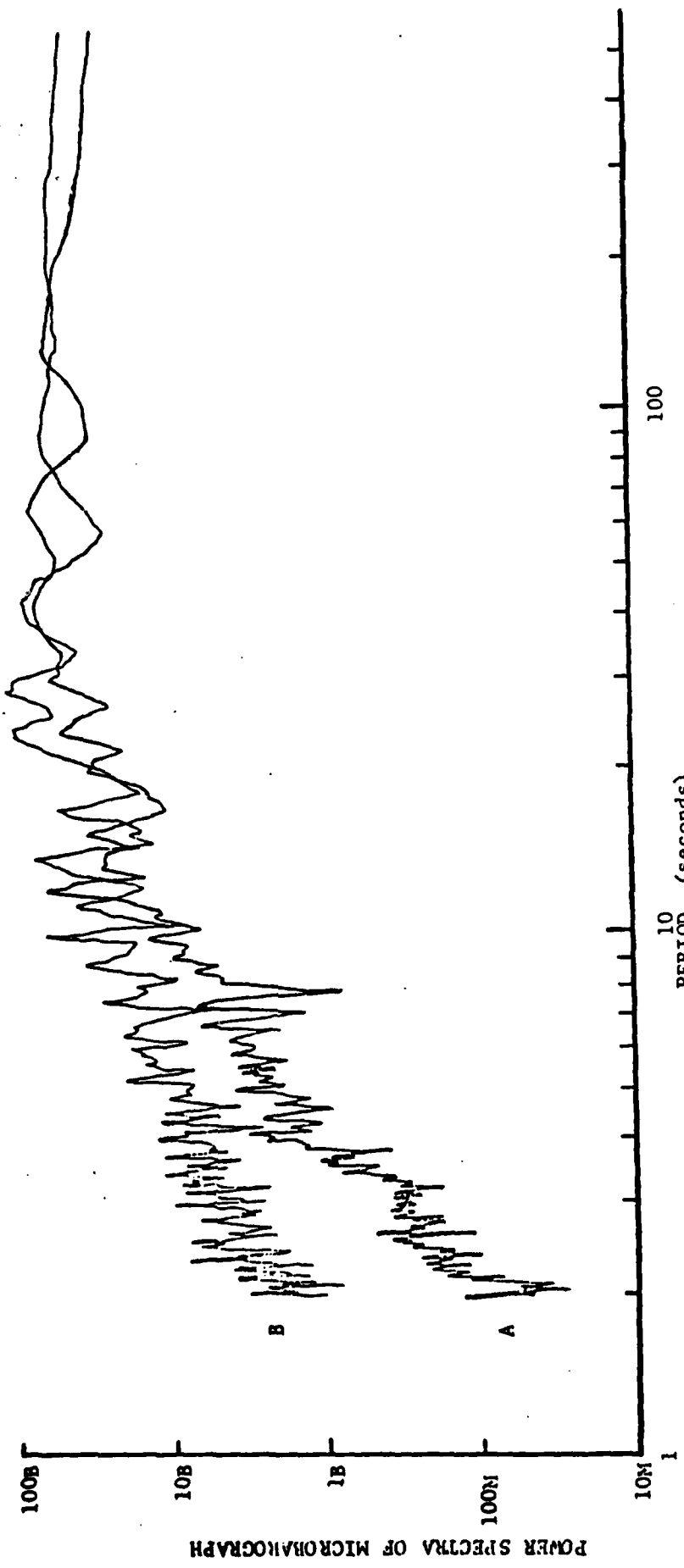

Fig. 9(a). Comparison of power spectra of microbarograph of periods with mean speed approximately 5.7 m/s but different standard deviation.
period A V=5.77 m/s, S.D.=0.60 predictability=0.786
period B V=5.69 m/s, S.D.=0.88 predictability=0.519

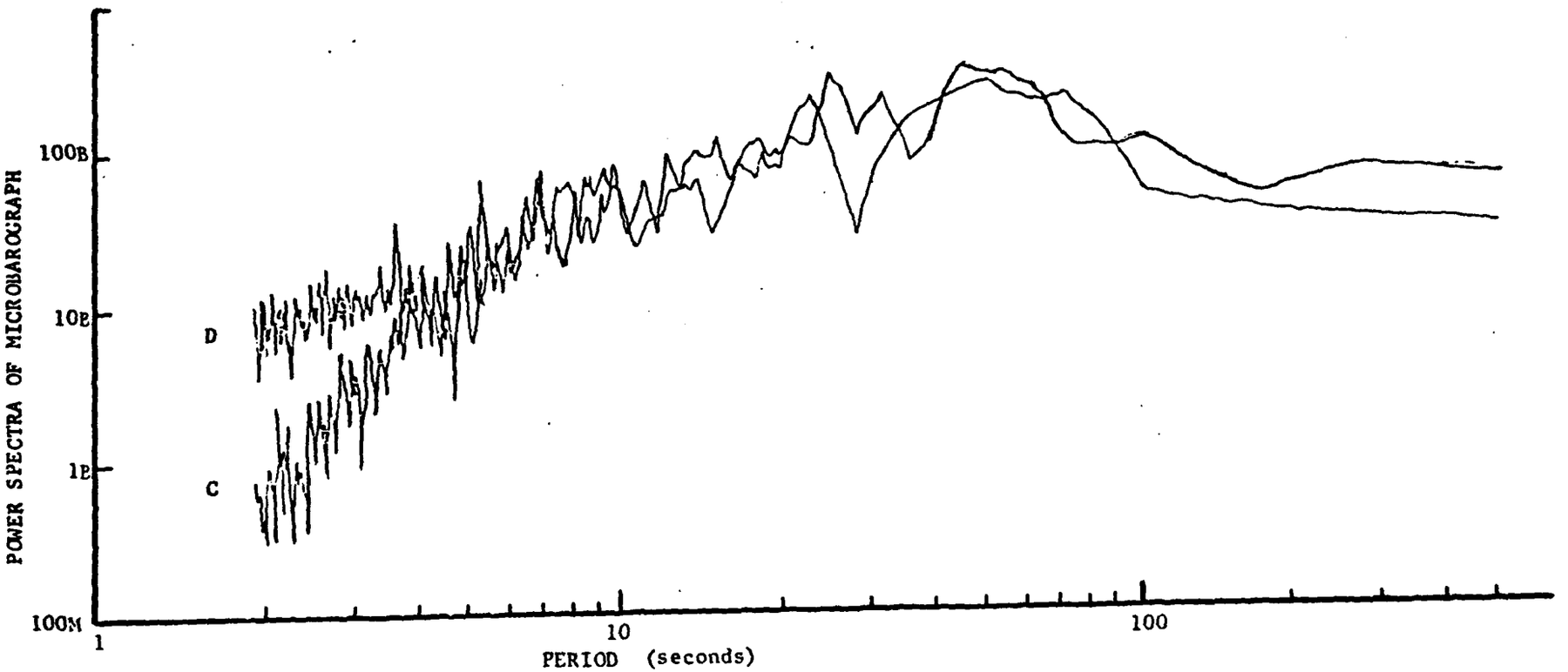

Fig. 9(b). Similar comparison of power spectra when mean wind speed about 6.5 m/s.
period C V= 6.29 m/s S.D.=0.97 predictability=0.807
period D V=6.86 m/s S.D.=1.12 predictability=0.668

increasing variance of wind speed.

Now let us take a look at the mathematical representation of the process. For any two time series, a function can be found such that

$$S(t) = \text{Function } (P(t))$$

where S(t) is the seismic noise data and P(t) is the microbarograph data as we used in the previous section. The function can be expanded in a polynomial form,

$$\begin{aligned} S(t) &= a_1 P(t) + a_2 P(t)^2 + a_3 P(t)^3 + \ldots\ldots \\ &= a_1 P(t) + \text{higher order terms} \\ &= f_1(t) + f_2(t) \end{aligned}$$

with $f_1(t) = a_1 P(t)$ which is linearly related to S(t) and $f_2(t)$ are the higher order terms which are not linearly related to S(t).

After taking Fourier transforms, we get

$$S(f) = F_1(f) + F_2(f).$$

In our experiment, $F_1(f)$ is primarily the energy in the period range 20 to 100 seconds because of the linear dependence existing between S(t) and P(t) in this range. $F_2(t)$ is then the higher order high frequency portion for which Wiener filtering is ineffective. During the intervals with steady wind, $F_2(f)$ is small enough to be neglected. The linear transfer function between the time series S(t) and P(t) is

essentially the linear part $f_1(t)$ and we expect very good prediction of the noise energy on the seismogram. Once the high frequency energy increases due to the breaking down of the turbulent cells to small eddies, the nonlinear energy $F_2(f)$ increases (Fig. 9) and dominates the whole process. The linear filter is then working on a non-linear system and thus fails to predict noise accurately.

CONCLUSION

Most of the noise recorded on the long-period seismograph appears to be generated locally by pressure disturbances in the atmosphere moving at the mean wind speed. There is a component of the seismic noise field which is linearly related to the atmospheric pressure field in the period range 20 to 100 seconds. An optimum Wiener filter is designed to predict and reduce the wind noise by assuming that the nonlinear part within the period range is small and can be neglected. During intervals with unsteady meteorological conditions the turbulent cells are believed to break down into small eddies which increase the amount of high frequency energy and lead to a significant non-linear component in the relation between the pressure field and seismic noise in the period range 20 to 100 seconds. Thus the linear Wiener filter fails in noise prediction for time periods in which the wind speed is highly variable. Some other technique, such as deep burial of the seismometers is required to suppress the pressure generated noise under these conditions. For areas characterized by high and/or steady wind, Wiener filtering should be a useful tool for decreasing background seismic noise on long period (20-100 sec) surface instruments.

APPENDIX

Descriptions of the program names used in Fig. 3.

DISPLAY: This program can show simultaneously any three seismograms on the computer scope.

RAYTHEON: This program reads from a Raytheon TC 200 Field tape and converts the data to TAPE I/O (1025) format.

COORS: The program computes the distance and azimuth between reference points.

PLOT TAPE I/O: This program plots up to 13 blocks of a channel on a data tape with TAPE I/O (1025) format.

REFERENCES

Burg, J. P., 1964. Three-dimensional filtering with an array of seismometers. Geophysics, 29, p. 693-713.

Capon, J., 1969. Investigation of long-period noise at the Large Aperture Seismic Array. JGR, 74, p. 3182-3194.

Crary, A.P. & M. Ewing, 1952. On a barometric disturbance recorded on a vertical long-period seismograph. Trans. Am. Geophys. Un., 33, p. 499-502.

Douze, E. J. & G. G. Sorrells, 1975. Prediction of pressure generated earth motion using optimum filters. Bull. Seism. Soc. Amer., 65, No. 3, p. 637-650.

Ewing, M. & F. Press, 1953. Further study of atmospheric pressure fluctuations recorded on seismographs. Trans. Am. Geophys. Un., 34, p. 95-100.

Haubrich, R. A. & G. S. MacKenzie, 1965. Earth noise, 5 to 500 millicycles per second. 2, Reaction of the earth to oceans and atmosphere. JGR, 70, p. 1429-1440.

Kanasewich, E. R., 1973. Time sequence analysis in geophysics. The University of Alberta Press.

Levinson, N., 1947. The Wiener RMS error criterion filter design and prediction. J. Math. and Phys., 25, No. 4.

McDonald, J. A., E. J. Douze & E. Herrin, 1971. The structure of atmospheric turbulence and its application to the design of pipe arrays. Geophys. J., 26, No. 1-4, p. 99-109.

McDonald, J. A. & E. Herrin, 1975. Properties of pressure fluctuations in an atmospheric boundary layer. Boundary Layer Meteorology, 8, p. 419-436.

Robinson, E. A., 1967. Statical communication and detection with special reference to digital data processing of radar and seismic signal.

Savino, J., K. McCamy & G. Hade, 1972. Structure in earth

Noise beyond twenty seconds - a window for earthquakes. Bull. Seism. Soc. Amer., 62, No. 1, p. 141-176.

Sorrells, G. G., 1971. A preliminary investigation into the relationship between long-period seismic noise and local fluctuations in the atmospheric pressure field. Geophys. J., 26, No. 1-4, p. 71-82.

Sorrells, G. G., J. A. McDonald, Z. A. Der & E. Herrin, 1971. Earth motion caused by local atmospheric pressure changes. Geophys. J., 26, No. 1-4, p. 83-98.

Sorrells, G. G. & T. T. Goforth, 1973. Low-frequency earth motion generated by slowly propagating partially organized pressure fields. Bull. Seism. Soc. Amer., 63, No. 5, p. 1583-1601.

Ziolkowski, A., 1973. Prediction and suppression of long-period nonpropagating seismic noise. Bull. Seism. Soc. Am., 63, No. 3, p. 937-958.